Supporting Information

for

In-situ Growth of MnO_2 Nanoparticles on Supramolecular Polyaniline as Chiral Nanozymes for Effective Enantioselective Catalysis

Chu Wang, Zheng Xi,* Xiaohuan Sun, Jie Han* and Rong Guo

School of Chemistry and Chemical Engineering, Yangzhou University, Yangzhou 225002, Jiangsu, P. R. China

**Corresponding author*

E-mails: xizheng@yzu.edu.cn (Z. X.); hanjie@yzu.edu.cn (J. H.)

1. Materials and characterization

Materials: Aniline monomer (Shanghai Chemical Co.) was distilled under reduced pressure before use. N-Phenyl-p-phenylenediamine, (1*R*)-(-)-Camphor-10-sulfonic acid (*R*-CSA), (1*S*)-(+)-Camphor-10-sulfonic acid (*S*-CSA), 3,4-dihydroxy-L-phenylalanine (*S*-DOPA), 3,4-dihydroxy-D-phenylalanine (*R*-DOPA) were purchased from Sigma-Aldrich. The H_2O_2, Potassium permanganate ($KMnO_4$), ammonium persulfate and ammonia were purchased from Sinopharm Chemical Reagent Co., Ltd. (Shanghai, China). MnO_2 nanoparticles were purchased from Borfos Nanotechnology Co., Ltd (Ningbo). All the above reagents were of analytical grade, and used without further purification. The water used in this study was deionized by milli-Q Plus system (Millipore, France), with the electrical resistivity of 18.2 MΩ.

Instruments and characterization: Morphologies of the as prepared nanomaterials were characterized with field emission scanning electron microscope (FESEM, 300, ZEISS), transmission electron microscope (TEM, HT7800) and high-resolution TEM (HRTEM, Tecnai G2 F30 S-Twin TEM, FEI). The UV-Vis absorption spectra were recorded using UV-2550 UV/Visible spectrophotometer (JASCO International Co., Ltd.). The CD analysis was performed on a JascoJ-810 CD spectropolarimeter (JASCO International Co., Ltd.) with a resolution of 1 nm. The phase composition was measured using an Axis Ultra X-ray photoelectron spectroscope (XPS, Kratos Analytical Ltd.) equipped with a standard monochromatic Al Kα source (hv = 1486.6 eV).

2. Synthesis of *P/M*-PANI: The *P/M*-PANI-*S/R*-CSA was prepared according to the previous publication. Specifically, 0.2 g (2.1 mmol) of aniline, 3.235 g of *S/R*-CSA (13.9 mmol), and 0.063 mmol of oligomer were dissolved in 1.5 mL of water. Subsequently, the aqueous solution of ammonium persulfate (2.1 mmol) was added incrementally in five separate portions to the mixture of aniline and CSA. After each addition, the mixed solution was stirring vigorously for 30 s. The reaction mixture was left standing for 20 h at room temperature following by 3 times wash with water. Then the *P/M*-PANI-*S/R*-CSA were dispersed into 150 mL of 0.1 M $NH_3 \cdot H_2O$, stirring at room temperature for 4 h to obtain *P/M*-PANI for further use.

3. Synthesis of *P/M*-P@M(*x*): In a typical synthesis, $KMnO_4$ aqueous solution (0.02 mol L^{-1}) was mixed with aqueous solution containing *P/M*-PANI nanofibers (2.0 g L^{-1}). The total volume of the reaction system was maintained at 20 mL, the concentration of *P/M*-PANI nanofibers was set at 0.4 g L^{-1}, and the concentration of $KMnO_4$ ranged from 5 to 80 mmol L^{-1}. Then the reaction system was maintained under magnetic stirring at room temperature for 1.5 h. Finally, the products were washed with deionized water for 3 times and dispersed in 4 mL deionized water for further use.

4. Synthesis of *P/M*-P+M(45): In a typical synthesis, 8 mg of *P*-PANI or *M*-PANI were dispersed into 10 mL deionized water, respectively, and 10 mL of 1 M thioglycolic acid (TA) solution was added to the solution of *P*-PANI or *M*-PANI. After stirring for 4 h at room temperature, the *P*-PANI-TA and *M*-PANI-TA were collected by centrifugation

after washing three times with deionized water. Following, 16 mL MnO_2 NPs aqueous solution was mixed with 4 mL aqueous solution containing *P*-PANI-TA or *M*-PANI-TA nanofibers under stirring. Finally, the products were washed with deionized water for 3 times and dispersed in 4 mL deionized water for further use.

5. Kinetic measurements: Kinetic measurements were carried out in time course mode by monitoring the absorbance changes of reaction mixture at 475 nm. Experiments were carried out using 150 μL *P/M*-P@M(*x*) solution in a reaction volume of 3 mL buffer solution (25 mM Na_2HPO_4, pH 7.0, 37 ℃) with DOPA as substrate, and the concentration of H_2O_2 was kept at 50 mM. The oxidation rates of *R/S*-DOPA in the presence of chiral nanozymes were analyzed according to the Michaelis-Menten model: $v = V_{max}C/(K_M+C)$, where v is the initial velocity, V_{max} is the maximal reaction velocity, K_M is the affinity constant, and C is the concentration of substrate. The v at the determined concentration is calculated according to Lambert Beer's law: $v = A\cdot\varepsilon^{-1}\cdot L^{-1}\cdot t^{-1}$, where A is the absorbance changes at λ_{max} = 475 nm (ε = 4770 $M^{-1}\cdot cm^{-1}$) of the dopachrome products for *R/S*-DOPA, L is the optical length of the cuvette, and t is the time corresponding to the absorbance changes. k_{cat} was calculated according to the equation: $k_{cat} = V_{max}/S$, where S is the mass of the chiral nanozyme used in the reaction system. Select factor of various nanocatalysts for *R/S*-DOPA was defined as $[k_{cat}/K_M]_{S\text{-DOPA}}/[k_{cat}/K_M]_{R\text{-DOPA}}$ or $[k_{cat}/K_M]_{R\text{-DOPA}}/[k_{cat}/K_M]_{S\text{-DOPA}}$, respectively.

6. Measurement of activation energy: The activation energies (E_a) for the DOPA

catalytic reaction taking advantage of *P/M*-P@M(*x*) was calculated according to Arrhenius equation:

$$\ln v = \ln A - E_a/RT \quad \text{(Eq. S1)}$$

where *A*, is constant, is the frequency factor, *R* is the gas constant and *T* is the absolute temperature (K). When measuring the E_a, the concentration of H_2O_2 and DOPA were kept at 50 mM and 0.05 mM, respectively.

7. Enantioselective separation of DOPA: 20.0 mg of *P/M*-P@M(*x*) was mixed with 5 mL of racemic DOPA aqueous solution (0.05 mM). The suspension was stirred for 4 h. After that, the suspension was filtered, and the filtrate was diluted and monitored by CD and UV.

8. Statistical analysis: The experimental results were expressed as mean ± SD.

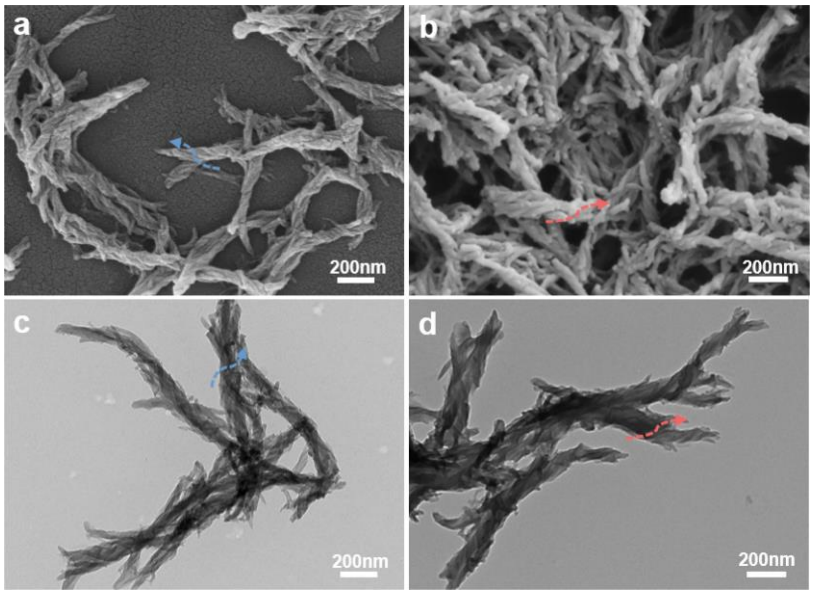

Fig. S1 SEM images of a) *P*-PANI and b) *M*-PANI, TEM images of c) *P*-PANI and d) *M*-PANI.

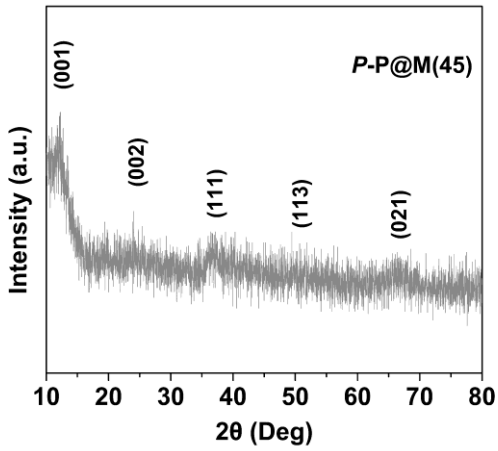

Fig. S2 XRD pattern of *P*-P@M(45).

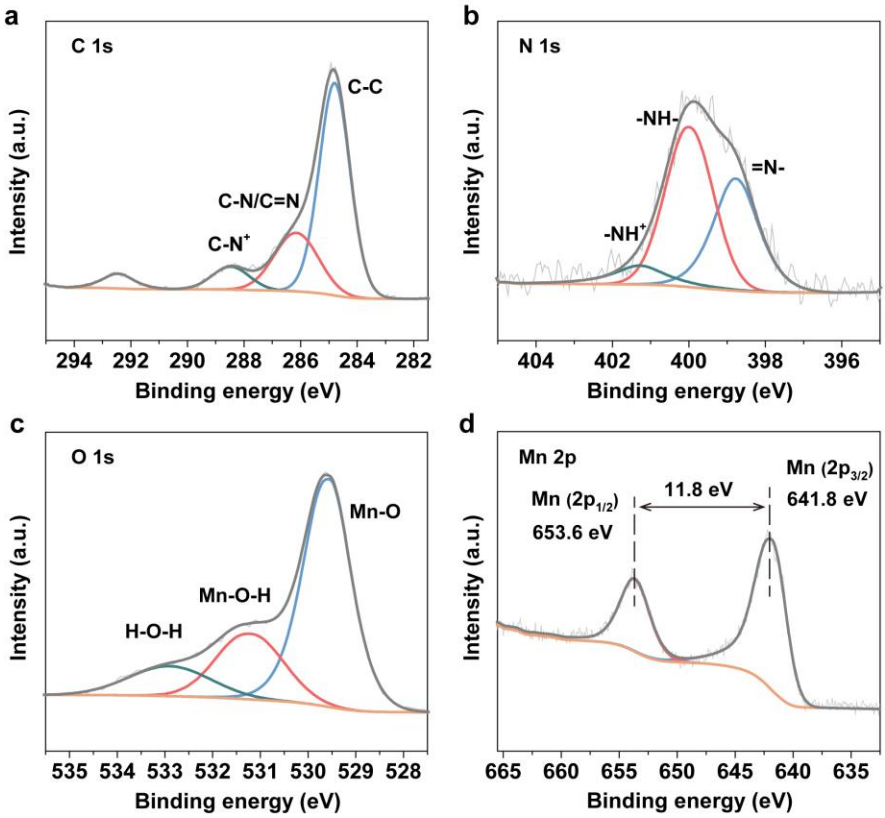

Fig. S3 XPS spectroscopy analysis of a) C 1s, b) N 1s, c) O 1s and d) Mn 2p for *P*-P@M(45).

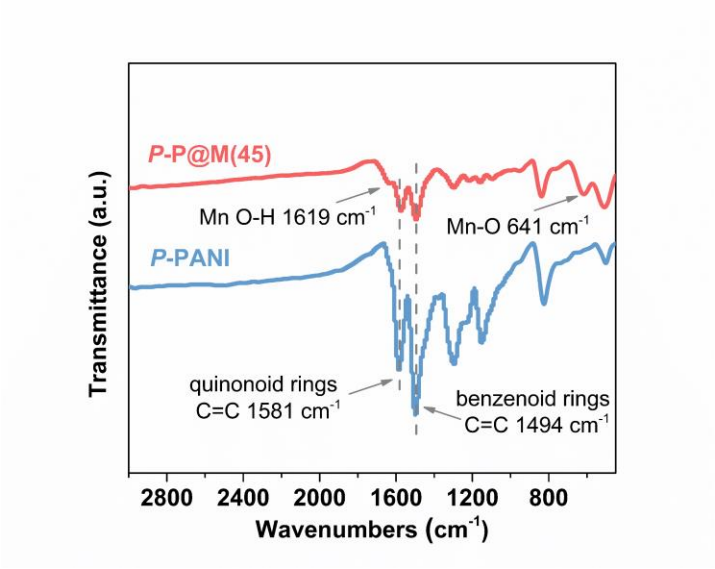

Fig. S4 FTIR spectra of *P*-PANI and *P*-P@M(45).

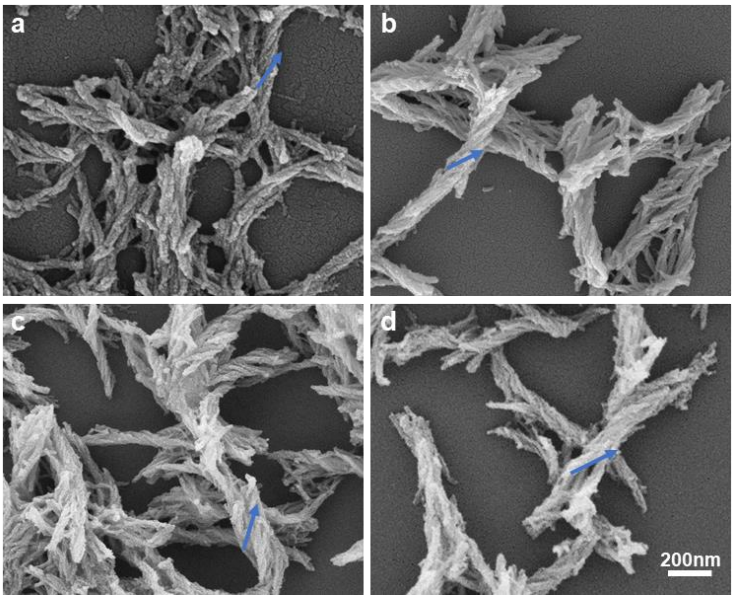

Fig. S5 SEM images of a) *P*-P@M(12), b) *P*-P@M(20), c) *P*-P@M(33) and d) *P*-P@M(45).

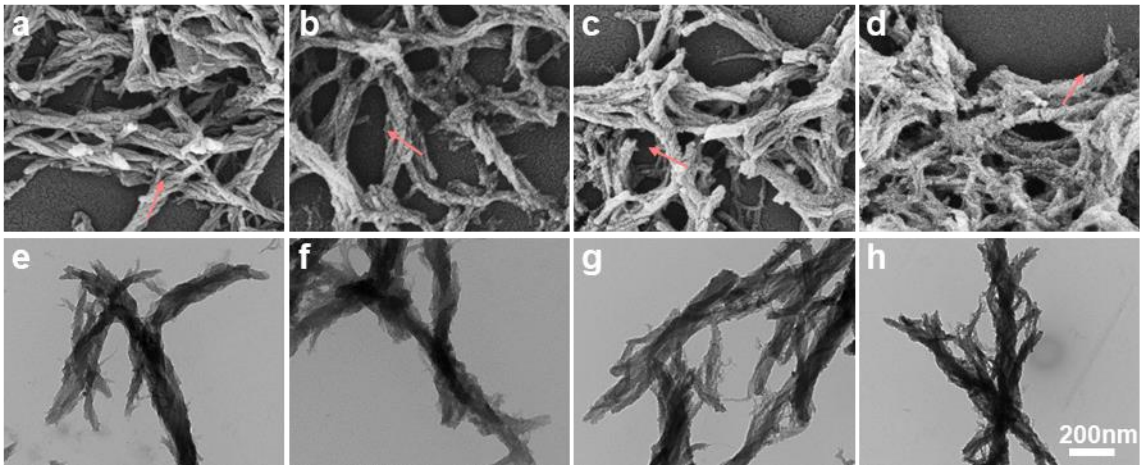

Fig. S6 SEM images of a) *M*-P@M(12), b) *M*-P@M(20), c) *M*-P@M(33) and d) *M*-P@M(45). TEM images of e) *M*-P@M(12), f) *M*-P@M(20), g) *M*-P@M(33) and h) *M*-P@M(45).

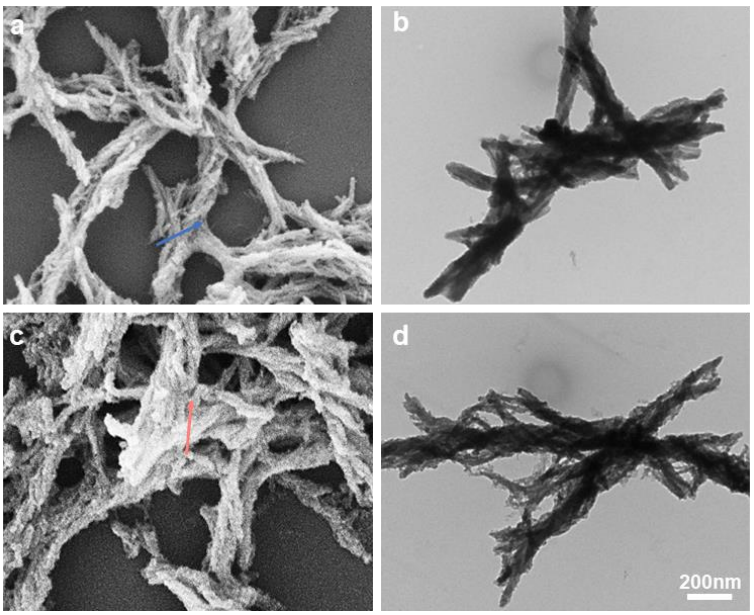

Fig. S7 a) SEM and b) TEM images of *P*-P@M(48). c) SEM and d) TEM images of *M*-P@M(48).

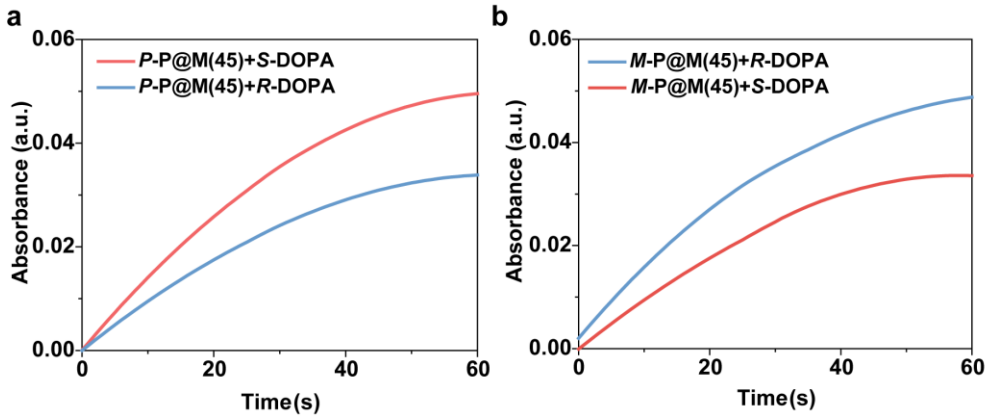

Fig. S8 Kinetic curves of "Absorption vs. Time" for a) *P*-P@M(45) and b) *M*-P@M(45) obtained with *S/R*-DOPA concentration fixed as 0.05 mM at λ_{max} = 475 nm.

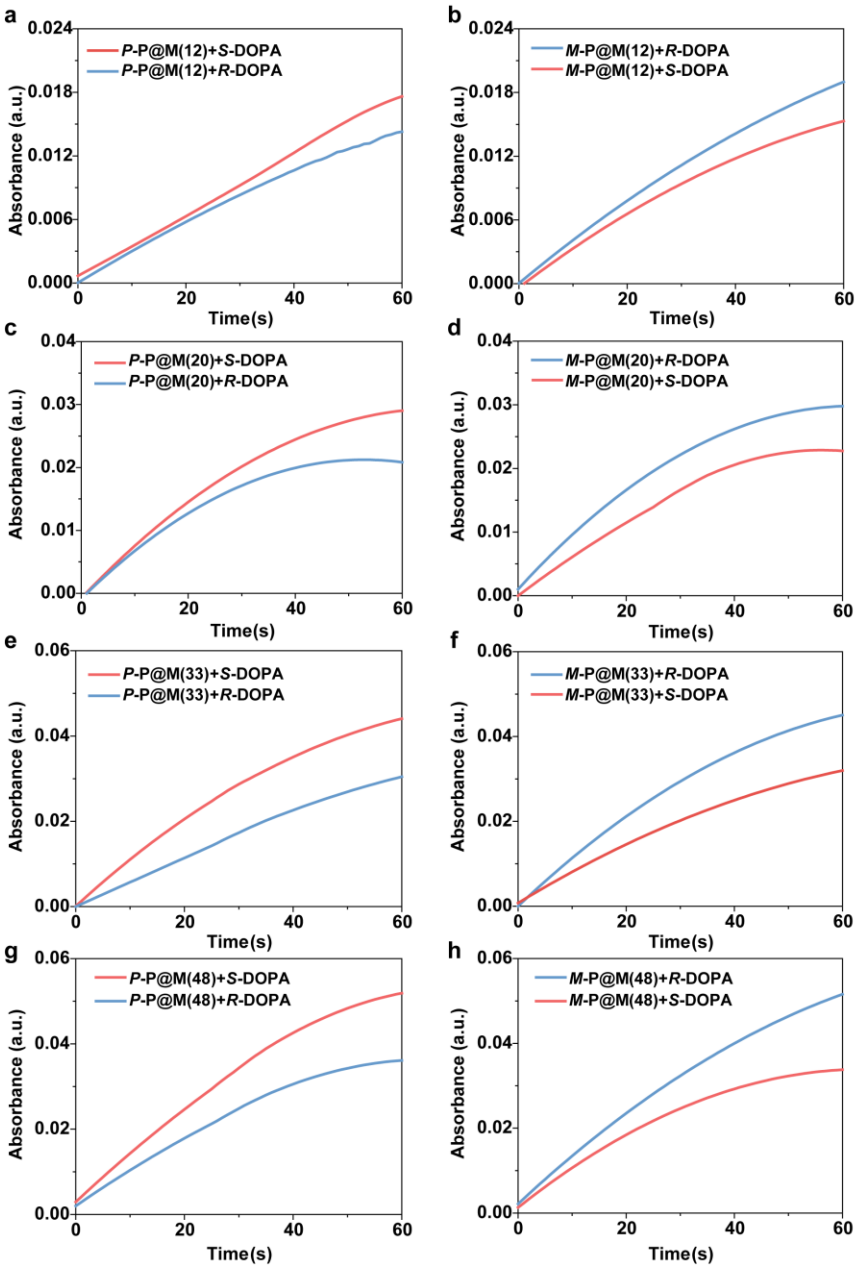

Fig. S9 Kinetic curves of "Absorption vs. Time" for a) *P*-P@M(12), b) *M*-P@M(12), c) *P*-P@M(20), d) *M*-P@M(20), e) *P*-P@M(33), f) *M*-P@M(33), g) *P*-P@M(48) and h) *M*-P@M(48) obtained with *S/R*-DOPA concentration fixed as 0.05 mM at λ_{max} = 475 nm.

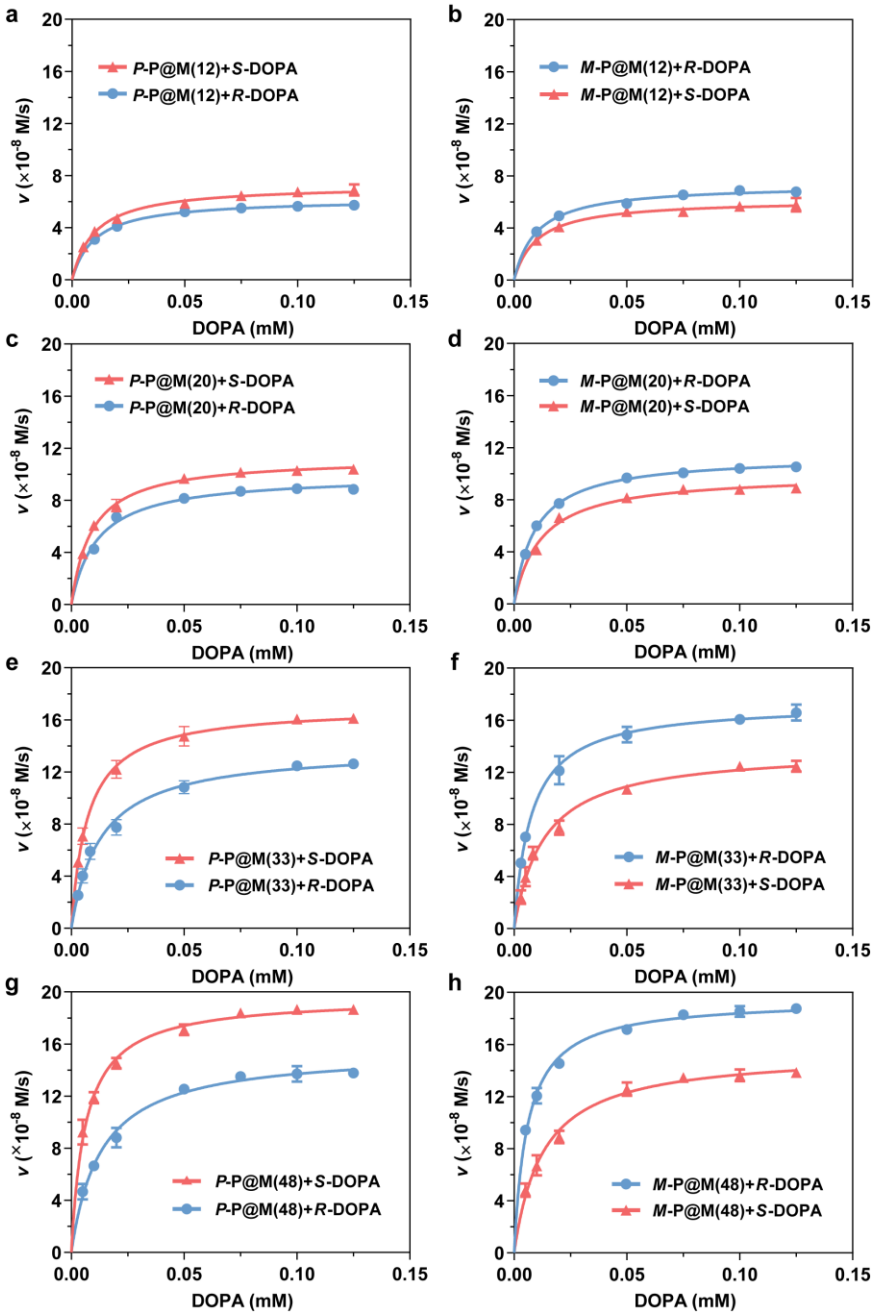

Fig. S10 Michaelis-Menten curves for the oxidation of *S*/*R*-DOPA catalysed by a) *P*-P@M(12), b) *M*-P@M(12), c) *P*-P@M(20), d) *M*-P@M(20), e) *P*-P@M(33), f) *M*-P@M(33), g) *P*-P@M(48) and h) *M*-P@M(48).

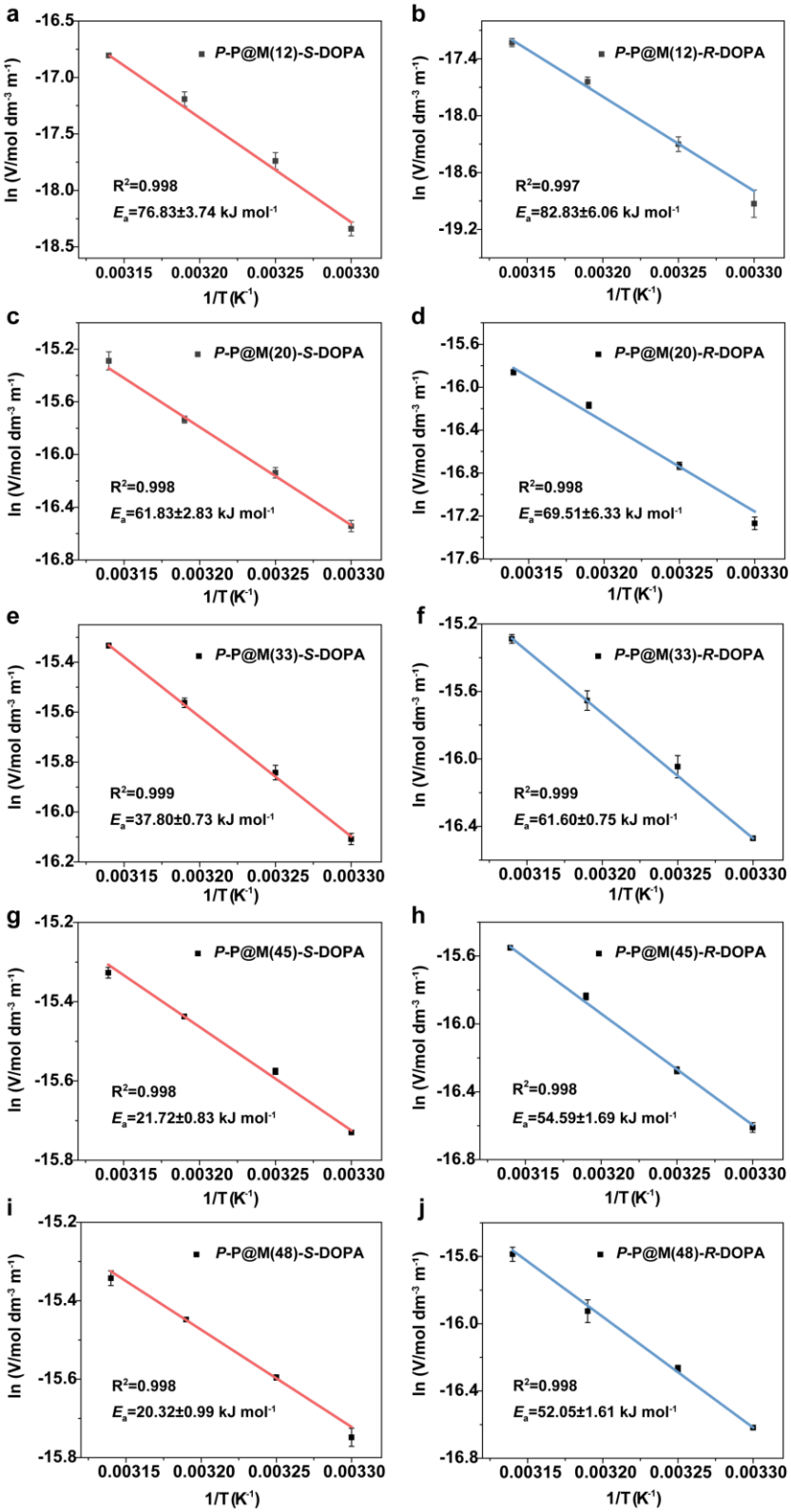

Fig. S11 Activation energy (E_a) lines for a, b) *P*-P@M(12), c, d) *P*-P@M(20), e, f) *P*-P@M(33) g, h) *P*-P@M(45) and i, j) *P*-P@M(48) for catalyzing *S/R*-DOPA.

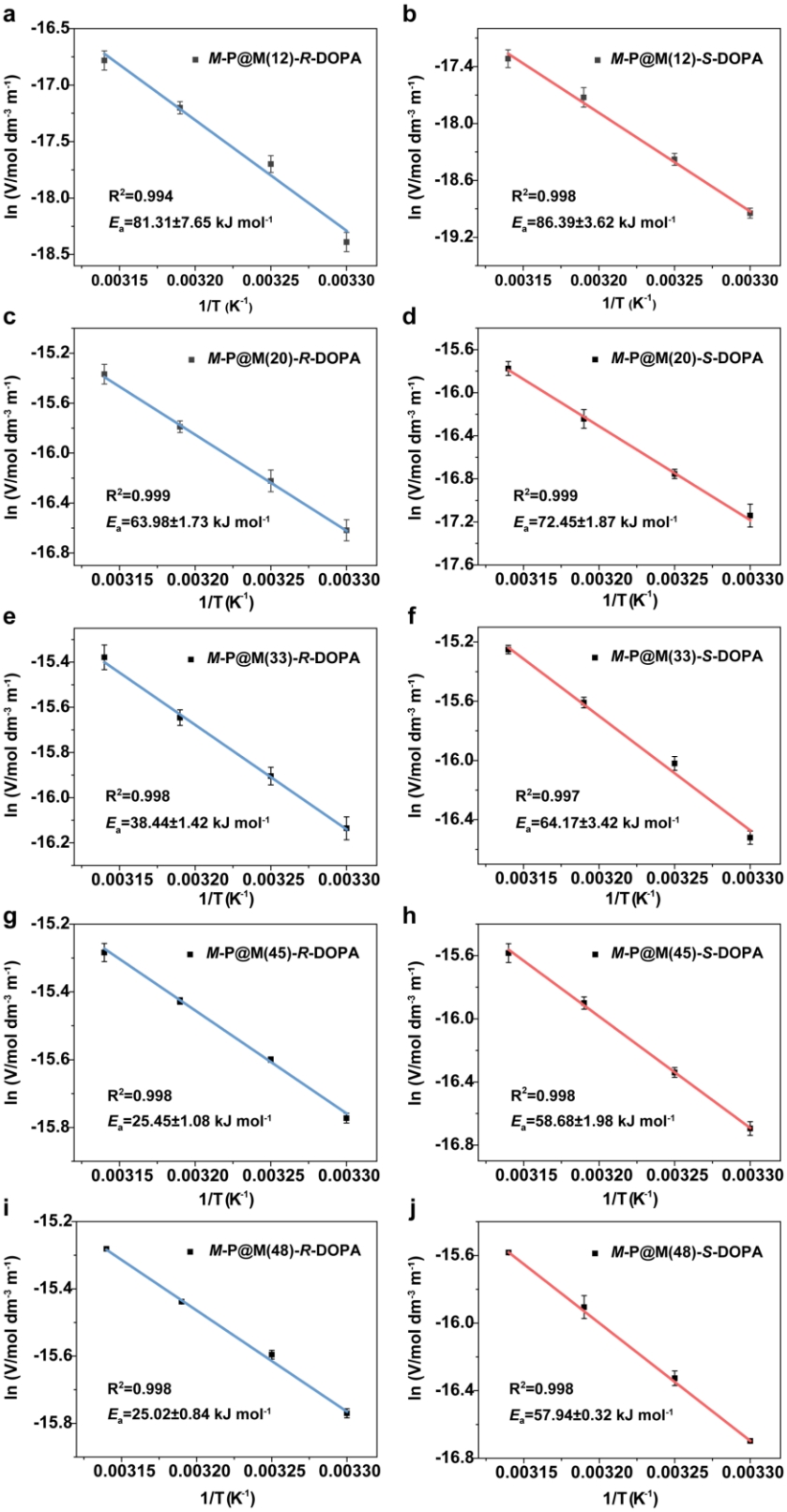

Fig. S12 Activation energy (E_a) lines for a, b) *M*-P@M(12), c, d) *M*-P@M(20), e, f) *M*-P@M(33), g, h) *M*-P@M(45) and i, j) *M*-P@M(48) for catalyzing *R/S*-DOPA.

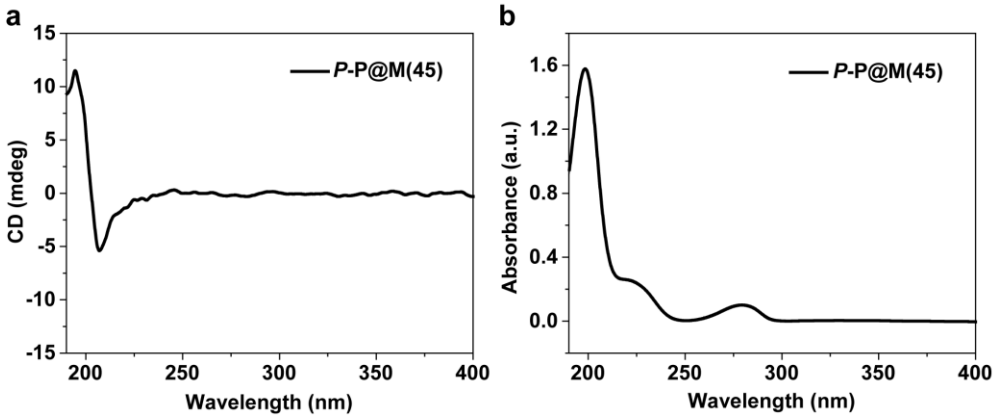

Fig. S13 a) The CD and b) UV-vis spectra for the 0.05 mM racemic DOPA solution after the *P*-P@M(45) absorption.

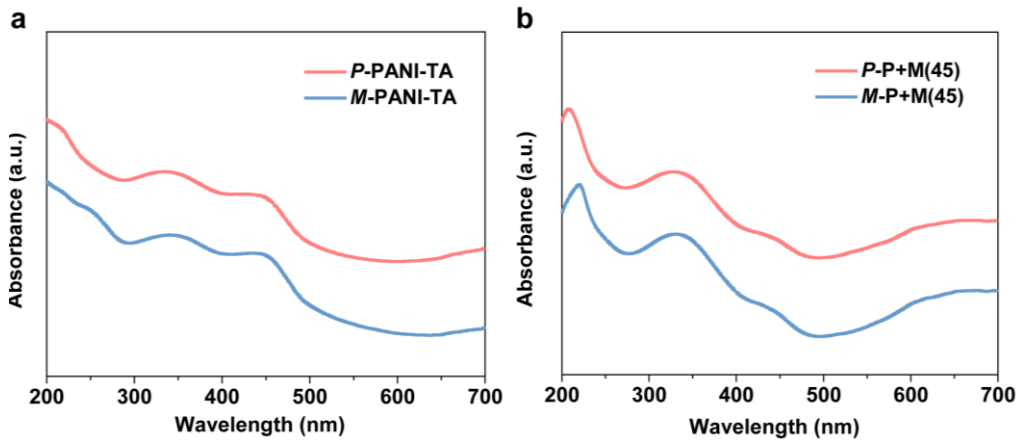

Fig. S14 The UV-vis spectra for a) *P/M*-PANI-TA and b) *P/M*-P+M(45).

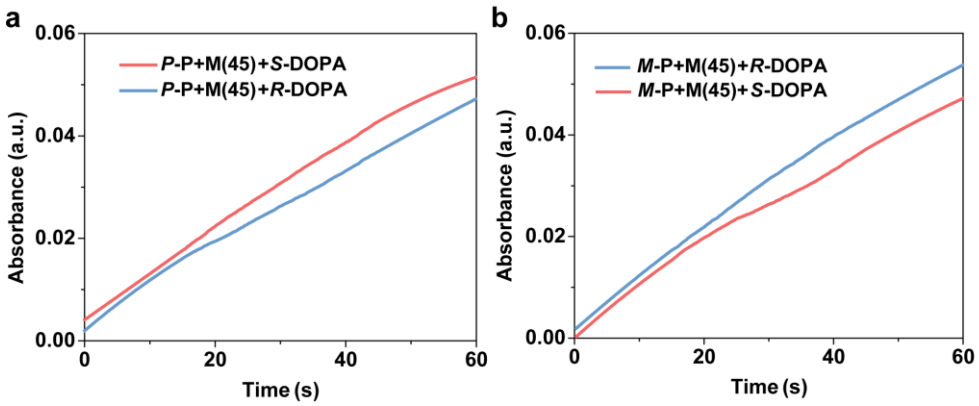

Fig. S15 Kinetic curves of "Absorption vs. Time" for a) *P*-P+M(45) and b) *M*-P+M(45) obtained with *S*/*R*-DOPA concentration fixed as 0.05 mM at λ_{max} = 475 nm.

Table S1 Weight percentage of MnO_2 in different samples calculated by ICP-AES analysis.

Sample	Sample concentration ($mg \cdot mL^{-1}$)	Mn concentration ($mg \cdot L^{-1}$)	Weight percentage of MnO_2 (%)
P-P@M(12)	0.50	39.01	12.33
P-P@M(20)	0.50	64.05	20.24
P-P@M(33)	0.50	104.0	32.87
P-P@M(45)	0.50	142.9	45.15
P-P@M(48)	0.50	152.5	48.21

Table S2 Kinetic parameters for enzymatic catalysis of *R*/*S*-DOPA enantiomers by *P*-P@M(12), *P*-P@M(20), *P*-P@M(33), *P*-P@M(45) and *P*-P@M(48).

Sample	Substrate	K_M (10^{-6} M)	k_{cat} (10^{-4} M·s^{-1}·g^{-1})	k_{cat}/K_M (s^{-1}·g^{-1})	Select factor
P-P@M(12)	*R*-DOPA	10.06±0.72	6.23±0.09	61.93±5.35	1.17±0.29
P-P@M(12)	*S*-DOPA	10.04±1.24	7.28±0.22	72.51±11.32	
P-P@M(20)	*R*-DOPA	11.49±1.61	9.41±0.32	81.90±14.55	1.51±0.40
P-P@M(20)	*S*-DOPA	9.10±0.58	11.29±0.17	124.07±9.82	
P-P@M(33)	*R*-DOPA	13.00±1.49	13.68±0.45	105.23±15.73	2.21±0.51
P-P@M(33)	*S*-DOPA	7.30±0.46	17.01±0.22	233.01±17.77	
P-P@M(45)	*R*-DOPA	13.80±0.92	14.98±0.21	108.55±8.80	2.82±0.41
P-P@M(45)	*S*-DOPA	6.28±0.32	19.24±0.20	306.37±18.84	
P-P@M(48)	*R*-DOPA	13.25±1.09	15.51±0.28	117.06±11.82	2.63±0.48
P-P@M(48)	*S*-DOPA	6.36±0.41	19.61±0.29	308.33±24.54	

Table S3 Kinetic parameters for enzymatic catalysis of *R*/*S*-DOPA enantiomers by *M*-P@M(12), *M*-P@M(20), *M*-P@M(33), *M*-P@M(45) and *M*-P@M(48).

Sample	Substrate	K_M (10^{-6} M)	k_{cat} (10^{-4} M·s^{-1}·g^{-1})	k_{cat}/K_M (s^{-1}·g^{-1})	Select factor
M-P@M(12)	*R*-DOPA	10.08±1.51	7.36±0.28	73.02±14.03	1.20±0.36
M-P@M(12)	*S*-DOPA	10.16±0.87	6.18±0.13	60.83±6.54	
M-P@M(20)	*R*-DOPA	9.36±0.42	11.38±0.12	121.58±6.75	1.46±0.35
M-P@M(20)	*S*-DOPA	11.94±1.67	9.97±0.32	83.50±14.65	
M-P@M(33)	*R*-DOPA	7.56±0.54	17.30±0.29	228.84±20.28	2.18±0.50
M-P@M(33)	*S*-DOPA	13.14±1.36	13.77±0.40	104.79±14.04	
M-P@M(45)	*R*-DOPA	6.25±0.21	19.34±0.13	309.44±12.49	2.75±0.30
M-P@M(45)	*S*-DOPA	13.21±0.72	14.85±0.19	112.41±7.59	
M-P@M(48)	*R*-DOPA	6.23±0.36	19.42±0.23	311.72±21.78	2.58±0.52
M-P@M(48)	*S*-DOPA	12.77±1.31	15.44±0.39	120.91±15.62	

Table S4 Comparison of the chiral nanozymes for enantioselective catalysis of *R/S*-DOPA measured in our work with those reported in previous literatures.

Nanozyme	Activity	Select factor	Reference
D-C-Dots	OXD	2.11	*Nano Lett.* **2022**, *22*, 7203
L-C-Dots	OXD	1.95	
D-Cys@AuNPs-EMSN	POD	1.47	*Angew. Chem. Int. Ed.* **2018**, *57*, 16791
L-Cys@AuNPs-EMSN	POD	1.69	
CeNP@D-Phe	OXD	1.13	*Chem.Eur. J.* **2017**, *23*, 18146
CeNP@L-Phe	OXD	1.87	
D-FexCuySe NPs	POD	1.49	*Nanotechnology* **2022**, *33*, 135503
L-FexCuySe NPs	POD	1.56	
D-His@Fe-COF	POD	1.51	*Mater. Horiz.* **2020**, *7*, 3291
L-His@Fe-COF	POD	1.86	
MOF-D-His-Cu	COs	2.12	*Nano Lett.* **2023**, *23*, 701
MOF-D-His-Cu	COs	2.19	
DCDH@CuNPs	POD	1.85	*ACS. Appl. Bio. Mater.* **2023**, *6*, 1676
AuNP@LIPIA 1	POD	1.90	*Nanoscale* **2020**, *12*, 2422
(*P*)-L-PhgC16-NR-M(ii)	POD	2.80	*Chem. Commun.* **2024**, *60*, 4569
(*M*)-L-PhgC16-NR-M(ii)	POD	2.35	
P-PANI-TA-M^{2+}	POD	2.07	*Small* **2023**, *19*, 2303739
M-PANI-TA-M^{2+}	POD	1.70	
***P*-P@M(45)**	**POD**	**2.82**	**This work**
***M*-P@M(45)**	**POD**	**2.75**	

Table S5 Kinetic parameters for enzymatic catalysis of *R*/*S*-DOPA enantiomers by *P/M*-P+M(45).

Sample	Substrate	K_M (10^{-6} M)	k_{cat} (10^{-4} M·s^{-1}·g^{-1})	k_{cat}/K_M (s^{-1}·g^{-1})	Select factor
P-P+M(45)	*R*-DOPA	25.51±3.28	20.62±0.90	80.83±14.16	1.28±0.39
P-P+M(45)	*S*-DOPA	20.32±1.93	21.07±0.54	103.69±12.62	
M-P+M(45)	*R*-DOPA	19.89±1.80	21.10±0.51	106.08±12.26	1.30±0.37
M-P+M(45)	*S*-DOPA	25.22±3.14	20.52±0.72	81.36±13.19	